

# Simulation and Analysis of A ZVT and ZCT Interleaved DC-DC Boost Converter

Kiruba.T , Santhi.M

ME. Power Electronics & Drives, Department of EEE, Sethu Institute Of Technology, Kariapatti, India.

ME. Power Electronics & Drives, Department of EEE, Sethu Institute Of Technology, Kariapatti, India.

**ABSTRACT**—In this paper, an interleaved boost converter with zero-voltage transition and zero-current transition characteristics is proposed. The interleaved approach reduces the ripple of the input current and output voltage. The active snubber cell provides main switch to turn ON with zero-voltage transition (ZVT) and to turn OFF with zero-current transition (ZCT). All semiconductor devices operate with soft switching. There is no additional voltage stress across the main and auxiliary components. The proposed converter has simple structure, minimum number of components, and ease of control. The operating principle and detailed steady-state analysis of the converter are given. The proposed converter is simulated using MATLAB/SIMULINK

**KEYWORDS**— soft switching, zero-voltage transition (ZVT), zero-current transition (ZCT), interleaved boost converter.

## I. INTRODUCTION

An Interleaved boost converter usually combines more than two conventional topologies and the current in the element of the interleaved boost converter is half of the conventional topology in the same power condition. Besides, the input current ripple and output voltage ripple of the interleaved boost converter are lower than those of the conventional topologies.

The single boost converter can use the zero-voltage transition (ZVT) and/or zero-current transition (ZCT) to reduce the switching loss at the high frequency switching [1]-[9]. High-Frequency PWM dc-dc converters have been widely used in power factor correction, battery charging, and renewable energy applications due to their high power density, fast response, and control simplicity. To achieve high-power density and smaller converter size, it is required to operate converters at high

switching frequencies. However, they are considered for the single topology. Many soft-switching techniques are introduced to the interleaved boost converter. In [10] the Zero-current-switching performance is used to reduce the switching losses by using coupled inductors in the interleaved boost converter. The cost of the converter is increased due to the usage of the coupled inductors.

In [11], [12], [13] zero voltage switching (ZVS) and zero current switching (ZCS) characteristics is achieved for the main switches of the interleaved boost converter. The ZVS and ZCS can operate only at variable frequency control to regulate the output. This is undesirable since it complicates the control circuit and generates unwanted EMI harmonics especially under wide load variations. In some papers [14] only ZVT characteristics is alone achieved for the main switches of the interleaved boost converter.

This paper proposes an interleaved boost converter with an active Snubber cell is proposed. The active snubber cell provides both characteristics of zero-voltage transition during turn ON of the switch and zero-current transition during turn OFF of the switch. The proposed converter is the parallel of two boost converters with their driving signals stagger 180 and this makes the operation assumed symmetrical. The converter has simple structure, minimum number of components, and ease of control.

## II. OPERATION MODES AND ANALYSIS

### A. Definitions and Assumptions

Interleaved ZVT-ZCT PWM boost converter circuit is shown in Fig.1. In this circuit, input voltage source is  $V_i$ , output voltage is  $V_o$ ,  $L_F, L_{F1}$ , is main inductor,  $C_F$  is output filter capacitor, and  $D_F, D_{F1}$  is main diode. The

main switch  $S_1, S_3$  consist of a main transistor  $T_1, T_3$  and its body diode  $D_1, D_3$ . The snubber circuit shown with dashed line is formed by snubber inductor  $L_S, L_{S1}$  a snubber capacitor  $C_S, C_{S1}$  and auxiliary switch  $S_2, S_4$  consist of a transistor  $T_2, T_4$  and its body diode  $D_2, D_4$ . The capacitor  $C_r, C_{r1}$  is assumed to be the sum of the parasitic capacitor of  $T_1, T_3$  and the other parasitic capacitors incorporating it. In the proposed converter, it is not required to use an additional  $C_r$  capacitor.

### B. Operation Modes of the converter

In Fig. 2(a)-(k), the equivalent circuit diagram of the operation modes are given respectively. The pulse waveforms for switches are shown in Fig. 3. The detailed analysis of the proposed circuit is presented below.

**Mode 1** [ $t_0 < t < t_1$ ; Fig.2 (a)]: At the beginning of this mode the main diode  $D_F$  is in the ON state and the input current  $I_i$  flows through the main diode. The main transistor  $T_1$  and auxiliary transistor  $T_2$  are in OFF state. The initial voltage of the  $C_S$  determines the soft-switching range of the circuit. At  $t=t_0$ , a resonance starts between snubber inductance  $L_S$  and snubber capacitor  $C_S$ . Due to the resonance  $T_2$  current rises and  $D_F$  current falls. The rise rate of current is limited by the snubber inductance  $L_S$  connected serially to the auxiliary switch so that the turn ON of the auxiliary switch is provided with ZCS for this interval, the following equations can be written:

$$i_{LS} = (V_0 - V_{CS0}) \frac{\sin w_s(t-t_0)}{L_S w_s} \quad (1)$$

$$V_{CS} = V_0 - (V_0 - V_{CS0}) \cos w_s(t - t_0) \quad (2)$$

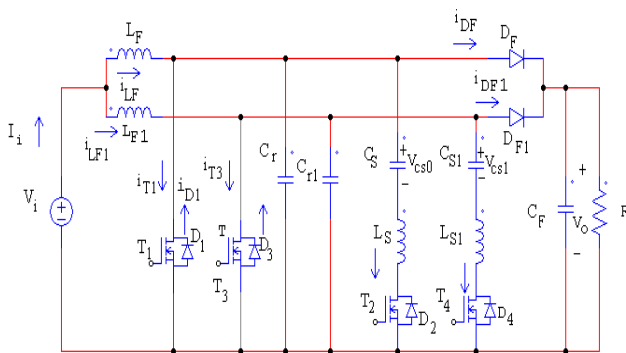


Fig.1 Circuit scheme of the proposed interleaved ZVT-ZCT boost converter.

In these equations

$$w_s = \sqrt{\frac{1}{L_S C_S}} \quad (3)$$

At  $t=t_1$ ,  $V_{CS}$  is charged to  $V_{CS1}$ ,  $i_{T2}$  reaches  $I_i$  and  $i_{DF}$  falls to zero. When  $i_{DF}$  reaches  $-I_{rr}$ ,  $D_F$  is turned OFF and this stage finishes.  $D_F$  is turned OFF with nearly ZCS and ZVS due to  $L_S$  and  $C_r$ . At the end of this mode

$$i_{LS} = i_{T2} = I_i + I_{rr} \quad (4)$$

$$V_{CS} = V_{CS1} \quad (5)$$

can be written.

**Mode 2** [ $t_1 < t < t_2$ ; Fig. 2(b)]: At the beginning of this mode the auxiliary transistor  $T_2$  is in the ON state and conducts the sum of the input current  $I_i$  and the reverse recovery current of  $D_F$ . A resonance between parasitic capacitor  $C_r, L_S, C_S$  starts. At  $t=t_2$ ,  $V_{cr}=0$ , diode  $D_1$  is turned ON with ZVS. The capacitor  $C_r$  is assumed the sum of the parasitic capacitor of  $T_1$  and the other parasitic capacitors incorporating it. At the end of this mode,

$$i_{LS} = i_{T2} = i_{LS2} \quad (6)$$

$$V_{CS} = V_{CS2} \quad (7)$$

are valid.

**Mode 3** [ $t_2 < t < t_3$ ; Fig. 2(c)]: At the beginning of this mode the resonant which is between the snubber inductance  $L_S$  and snubber capacitor  $C_S$  continues and diode  $D_1$  is turned ON and conducts the excess of snubber inductance  $L_S$  current from the input current. When control signal is applied to  $T_1$ ,  $D_1$  is in the ON state in order to provide ZVT turn ON of  $T_1$ . At  $t=t_3$ , this stage ends when the snubber inductance  $L_S$  current falls to input current and  $D_1$  is turned OFF under ZCS. At the end of this mode

$$i_{LS} = i_{T2} = i_{LS3} = I_i \quad (8)$$

$$V_{CS} = V_{CS3} \quad (9)$$

are valid.

**Mode 4** [ $t_3 < t < t_4$ ; Fig. 2(d)]: At the beginning of this mode, the main transistor is turned ON with ZVT and its current start to rise. The resonant between snubber

inductance  $L_S$  and snubber capacitor  $C_S$  continues. For this mode the following equation are derived:

$$i_{LS} = I_i \cos w_s (t - t_3) - \frac{V_{cs4}}{w_s L_S} \sin w_s (t - t_3) \quad (10)$$

$$V_{cs} = V_{cs4} \cos w_s (t - t_3) + L_S w_s I_i \sin w_s (t - t_3) \quad (11)$$

At  $t=t_4$ , the current in the main transistor reaches to the input current level and  $i_{LS}$  becomes zero hence the current through the auxiliary transistor reaches zero and  $T_2$  is turned OFF. At the end of this mode,

$$i_{LS} = i_{T2} = I_{LS4} = 0 \quad (12)$$

$$V_{cs} = V_{cs4} \quad (13)$$

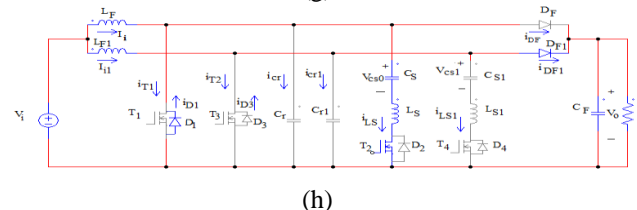
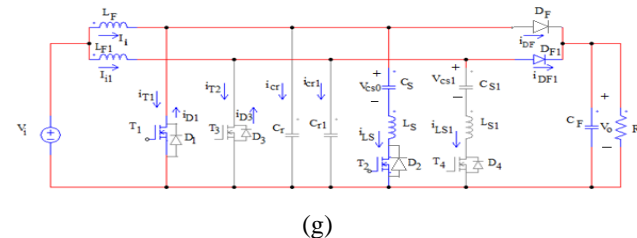
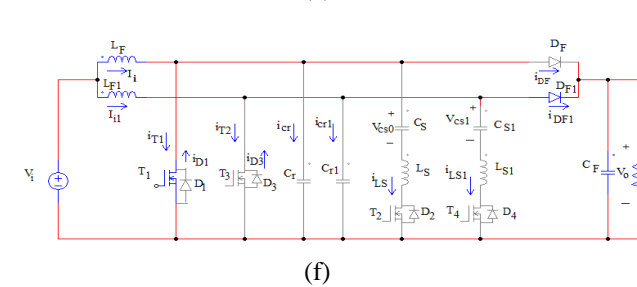
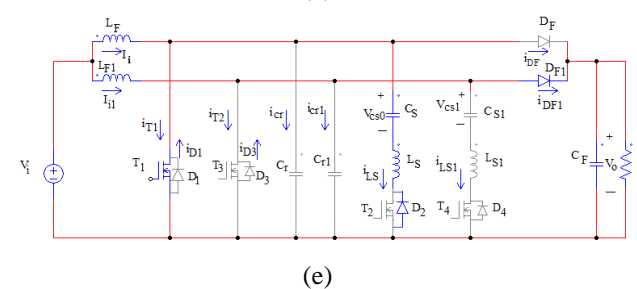
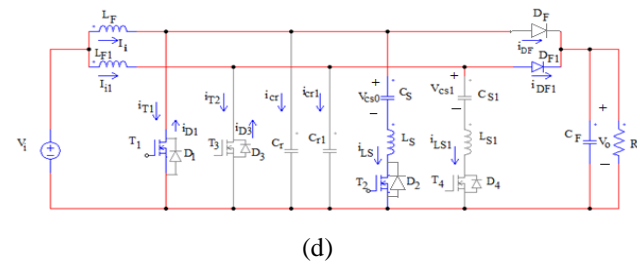
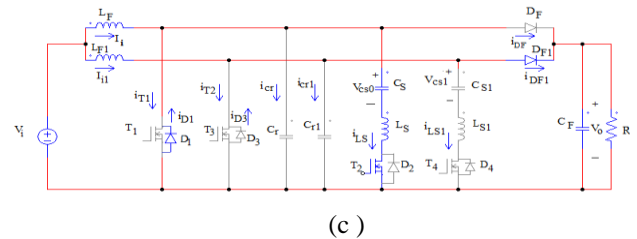
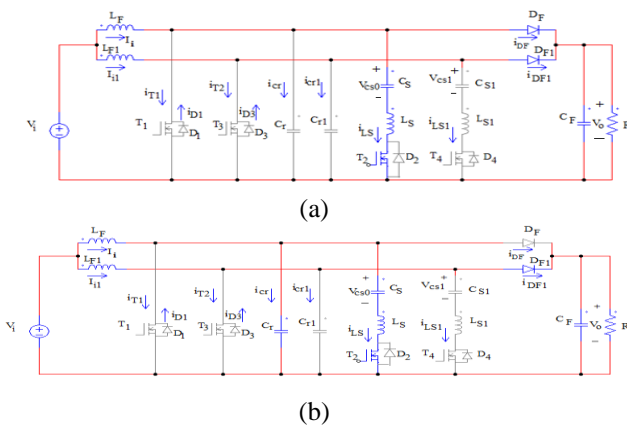
are valid.

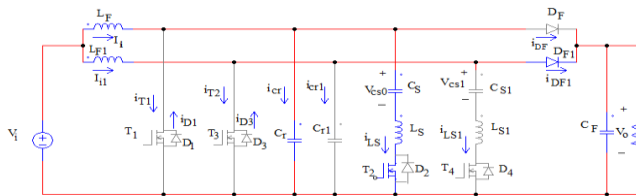
**Mode 5 [ $t_4 < t < t_5$  : Fig. 2(e)]:** In this mode the diode  $D_2$  is turned ON with ZCS and its current starts to rise. The resonant between snubber inductance and snubber capacitance continues. The current through snubber inductance  $i_{LS}$  becomes negative, so the current through the main transistor is higher than the input current in this mode. The equation is expressed as follows:

$$i_{LS} = -\frac{V_{cs4}}{w_s L_S} \sin w_s (t - t_4) \quad (14)$$

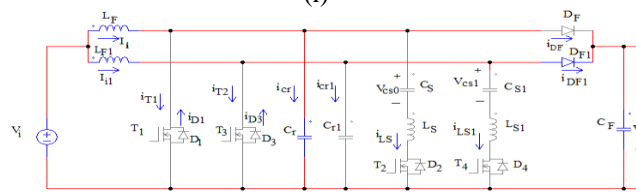
$$V_{cs} = V_{cs4} \cos w_s (t - t_4) \quad (15)$$

At  $t=t_5$ , the main transistor current decrease to the input current level and  $i_{LS}$  becomes zero.  $i_{D2}$  becomes zero and it is turned OFF under ZCS. At the end of this mode,

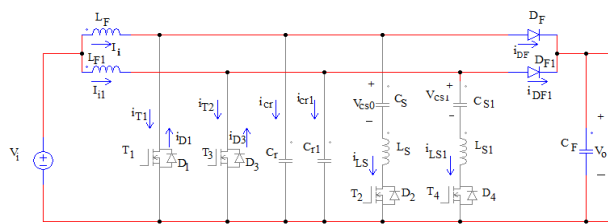




(i)



(j)



(k)

capacitor  $C_S$ . starts through  $C_S$ - $L_S$ - $T_2$ - $T_1$ . The equations can be expressed as follows,

$$i_{LS} = -\frac{V_{cs5}}{w_s L_S} \sin w_s (t - t_5) \quad (19)$$

$$V_{cs} = V_{cs5} \cos w_s (t - t_5) \quad (20)$$

The auxiliary transistor  $T_2$  is turned ON with ZCS due to the snubber inductance  $L_S$ . The main transistor  $T_1$  current falls with the rise in snubber inductance current. At  $t=t_7$ , when the current of  $T_2$  reaches to the input current level, the main transistor current becomes zero and this mode finishes. At the end of this mode,

$$i_{LS} = i_{T2} = I_{LS7} = I_i \quad (21)$$

$$V_{cs} = V_{cs7} \quad (22)$$

are valid

**Mode 8 [ $t_7 < t < t_8$ : Fig. 2(h)]:** At the beginning of this mode,  $D_1$  is turned ON with ZCS. If  $T_1$  turned OFF when  $D_1$  is ON,  $T_1$  turns OFF with ZVS and ZCS.  $D_1$  conducts the excess of  $i_{LS}$  from the input current. The resonance between  $L_S$  and  $C_S$  continues. At  $t=t_8$ ,  $i_{D1}$  reaches  $-I_{rr}$  and turns OFF, and this stage ends. At the end of this mode

$$i_{LS} = i_{T2} = I_{LS8} = I_i - I_{rr} \quad (23)$$

$$V_{cs} = V_{cs8} = V_{cs0} \quad (24)$$

are valid.

**Mode 9 [ $t_8 < t < t_9$ : Fig. 2(i)]:** In the beginning of this mode, a resonance between parasitic capacitor  $C_r$ , snubber inductor  $L_S$  and snubber capacitor  $C_S$  starts. At  $t=t_9$ ,  $i_{LS}$  falls to zero and the capacitor  $C_r$  is charged from zero to  $V_{cs8}$  with this resonance. The auxiliary transistor  $T_2$  is turned OFF with ZCS. At the end of this mode

$$i_{LS} = i_{T2} = I_{LS9} = 0 \quad (25)$$

$$V_{cs} = V_{cs9} = V_{cs0} \quad (26)$$

are valid.

**Mode 10 [ $t_9 < t < t_{10}$ : Fig. 2(j)]:** In this mode  $C_r$  is charged linearly under the input current. At instant  $t_{10}$   $C_r$  voltage reaches the output voltage  $V_o$ , and the main diode  $D_F$  is turned ON with ZVS.

**Mode 11 [ $t_{10} < t < t_{11}$ : Fig. 2(k)]:** This mode is the OFF state of the conventional boost converter. During this mode, the main diode  $D_F$  continues conducting the input

Fig. 2. Equivalent circuit schemes of the operation modes in the proposed novel ZVT-ZCT-PWM boost converter.

(a)  $t_0 < t < t_1$ . (b)  $t_1 < t < t_2$ . (c)  $t_2 < t < t_3$ . (d)  $t_3 < t < t_4$ . (e)  $t_4 < t < t_5$  (f)  $t_5 < t < t_6$ . (g)  $t_6 < t < t_7$ . (h)  $t_7 < t < t_8$ . (i)  $t_8 < t < t_9$ . (j)  $t_9 < t < t_{10}$ . (k)  $t_{10} < t < t_{11} = t_0$ .

$$i_{LS} = i_{T2} = I_{LS5} = 0 \quad (16)$$

$$V_{cs} = V_{cs5} \quad (17)$$

are valid.

**Mode 6 [ $t_5 < t < t_6$ : Fig. 2(f)]:** In this mode main transistor  $T_1$  conducts the input current  $I_i$  and snubber circuit is not active. This mode is the ON state of the conventional boost converter.

$$I_{T1} = I_i \quad (18)$$

are valid.

**Mode 7 [ $t_6 < t < t_7$ : Fig. 2(g)]:** In this mode the control signal is applied to auxiliary transistor  $T_2$ , a new resonance between snubber inductance  $L_S$  and snubber

current  $I_i$  and the snubber circuit is not active. For this mode

$$i_{DF} = I_i \quad (27)$$

can be written.

*Mode 12-22*: since two cells of the converter are identical and operating with the same frequency and duty cycles and there is only  $180^\circ$  phase shift between these two cells, the circuit behavior during operation modes of 11-22 is similar to that of during modes of 1-11. The circuit analysis of the converter during the last eleven modes is similar to that of the first eleven modes and can be Achieved by replacing  $T_1, T_2, D_1, D_2, D_F, L_F, C_r, L_S, C_S, V_{cs0}$  with  $T_3, T_4, D_3, D_4, D_{F1}, L_{F1}, C_{r1}, L_{S1}, C_{S1}, V_{cs1}$  respectively.

### III DESIGN PROCEDURE

The design procedure for the proposed interleaved ZVT-ZCT boost converter is presented in this section.

#### 1. Operating Requirements:

Output power $P_{out}$ :	1KW
Input voltage $V_{in}$ :	200V DC
Switching frequency ( $f_{sw}$ ):	100 KHZ
Output voltage ( $V_o$ ):	400V

#### 2. Input and Output Parameters:

The relationship between the duty cycle and the Output/input ratio for interleaved boost converter is

$$\frac{V_o}{V_{in}} = \frac{1}{1-D} \quad (28)$$

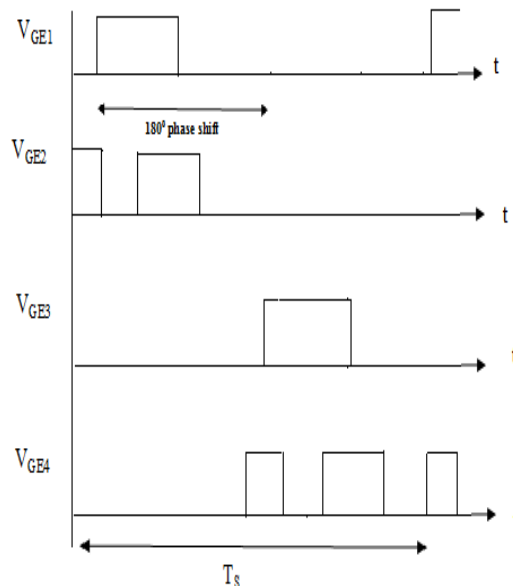


Fig. 3 Pulse waveforms for switches

#### 3. Inductor Current Ripple Peak-To-Peak Amplitude:

The inductor current ripple peak-peak amplitude is given by

$$\Delta I_{L1/2} = \frac{V_{in} D}{f_{sw} L} \quad (29)$$

Where  $f_{sw}$  is the switching frequency,  $D$  is the duty cycle,  $V_{in}$  is the input Voltage and  $L$  is the inductance.

#### 4. Output Voltage Ripple:

Since the load and output capacitor are supplied through two diodes  $D_F$  and  $D_{F1}$ , the frequency of the output ripple current is twice the switching frequency. This decreases the output ripple voltage  $\Delta V_o$ . The output capacitor is determined as,

$$C = \frac{V_o D_F}{R \Delta V_o} \quad (30)$$

#### 5. Selection of Snubber Inductor:

The snubber inductance can be selected to provide the following conditions with reference to [15]. Here,  $t_{r2}$  is rise time of the auxiliary switch.  $V_{cs1}$  is assumed constant in  $t_{r2}$  duration

$$\frac{V_o - V_{cs1}}{L_s} t_{r2} \leq I_{imax} \quad (31)$$

To turn ON auxiliary switch with ZCS, the required Series inductor  $L_s$  is calculated as,

$$L_s \geq \frac{400-150}{5} \cdot 2 \cdot 10^{-6} \geq 0.1mH \quad (32)$$

The value of  $L_s$  is selected as the smallest possible value as 1mH in order to decrease ZCT duration.

6. Selection of Snubber Capacitor:

The snubber capacitor  $C_s$  is determined depending on the transient intervals. The sum of the transient intervals is selected to be smaller than 20% of transient intervals is equal to the resonant period  $t_R$

$$t_R < T_s \cdot \left(\frac{20}{100}\right) \quad (33)$$

$$t_R = 2\pi\sqrt{L_s C_s} \quad (34)$$

The value of  $C_s$  is selected as  $33\mu F$  to obtain appropriate ZVT duration.

IV. SIMULATION RESULTS

The computer simulation of proposed converter is done using MATLAB/SIMULINK and the results are presented. The simulation result of the output voltage and output current are shown in Fig. 4. Soft switching in the auxiliary switch is shown in the Fig. 6. Fig. 7. Shows the Ripple content in the output voltage. Ripple content in the output voltage is low due to interleaving technique. Ripple content in the output voltage is calculated by finding the difference between peak-to-peak voltages. Due to reduce in the ripple content in the output voltage efficiency of the converter is increased.

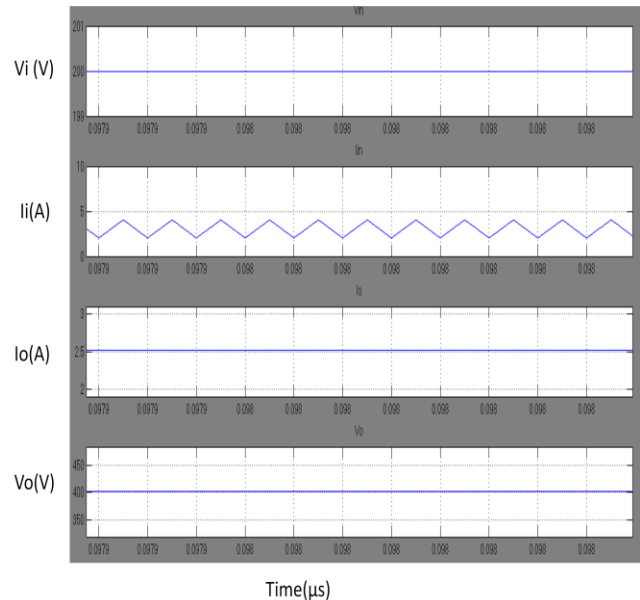


Fig.4 input and output voltage, current waveforms ( $V_{in}=200V$ ,  $I_i=5A$ ,  $V_{out}=400V$ ,  $I_{out}=2.5A$ )

Soft switching in the main switch is shown in the Fig.5 Comparisons of the output ripple voltage and THD of conventional ZVT-ZCT boost converter and interleaved ZVT-ZCT boost converter are shown in Table I.

Table I

TYPE	OUTPUT RIPPLE VOLTAGE	THD
ZVT-ZCT Boost Converter	32mV	105.65%
Interleaved ZVT-ZCT Boost Converter	2.8mV	76.02%



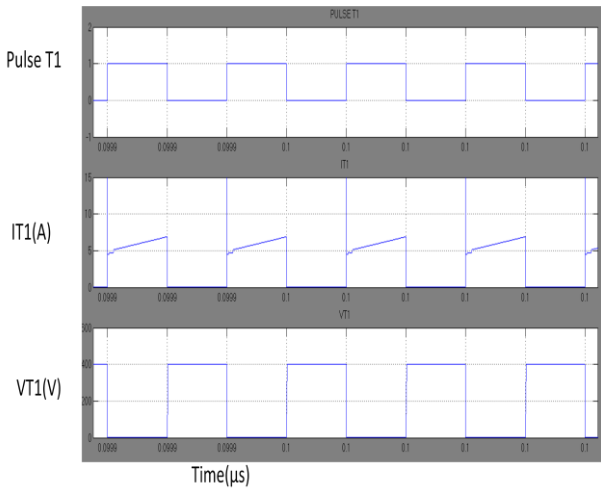


Fig.5 soft switching of the main switch

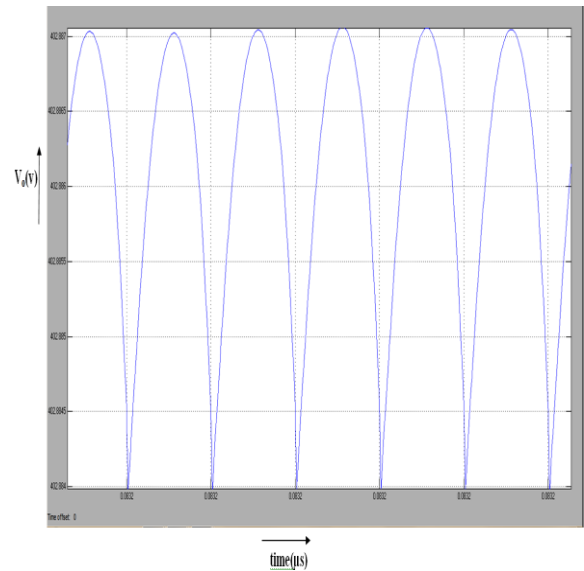


Fig.7 Ripple voltage waveform

Voltage across the main diode  $D_{F1}$ ,  $D_{F2}$  is shown in the Fig. 8 and Fig. 9.

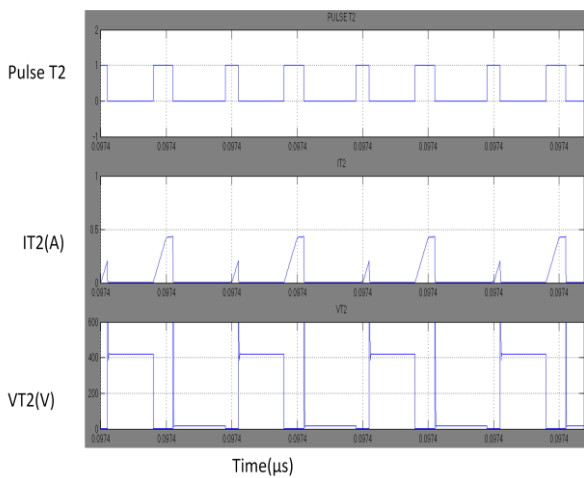


Fig.6 soft switching of the auxiliary switch

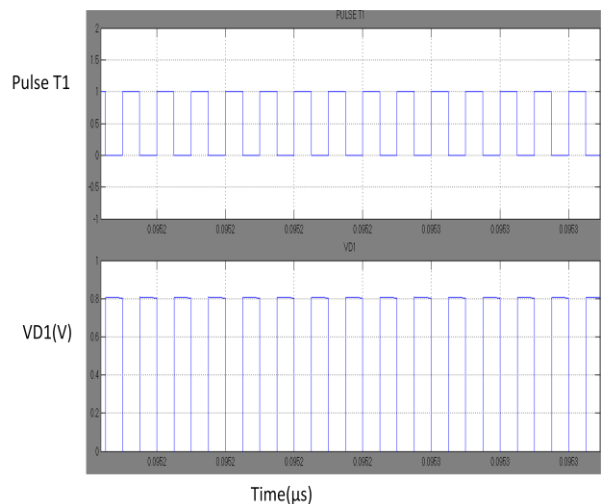


Fig. 8 pulse and voltage waveforms,  $T_1$ ,  $V_{DF1}$

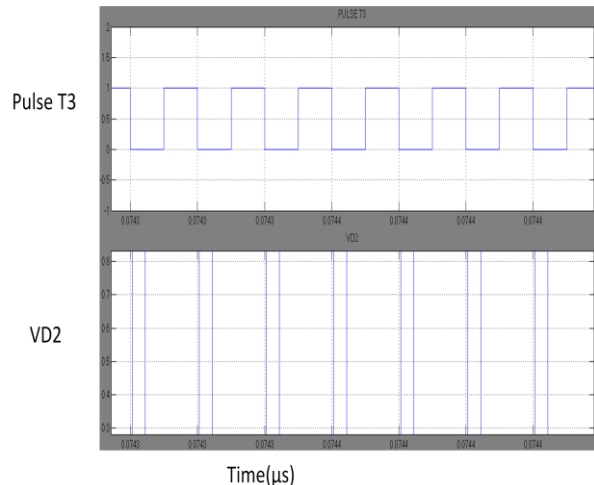


Fig. 9 pulse and voltage waveforms,  $T_2$ ,  $V_{DF2}$

## V. CONCLUSION

Interleaved ZVT-ZCT PWM boost converter is proposed in this paper. Hence, the input current ripple is reduced and the voltage stresses of the switches are greatly reduced compared with the conventional boost topology. This leads to the significant reduction of the conduction losses. Also, the switching losses is reduced by using an active snubber cell which provides ZVT turn on and ZCT turn OFF together for the main switch of the converter. Also, the proposed snubber cell is implemented by using only one quasi-resonant circuit without an important increase in cost and complexity. In the proposed converter, all semiconductor devices are switched under soft switching. The main diode is not subjected to any additional voltage and current stresses. The operation principles and steady-state analysis of the proposed converter are presented. The proposed converter is analyzed, design considerations are discussed, and its various operating modes are presented. The proposed converter was more efficient than the conventional boost converter.

## REFERENCES

- [1] Aksoy, A. F. Bakan, H. Bodur, and, "A novel ZVT-ZCT PWM DC-DC converter," in *Proc. 11<sup>th</sup> Eur. Conf. Power Electron. Appl.*, Sep. 2005, pp.1-8.
- [2] H. Bodur and A. F. Bakan, "A new ZVT-ZCT-PWM DC-DC converter," *IEEE Trans. Power Electron.*, vol. 19, no. 3, pp. 676-684, May 2004.
- [3] Nihan Altintas, A. Faruk Bakan, and Ismail Aksoy, "A Novel ZVT-ZCT-PWM Boost Converter" *IEEE Trans. Power Electron.*, vol. 20, no. 1, pp. 256-264, Jan. 2014.
- [4] D. Y. Lee, M. K. Lee, D. S. Hyun, and I. Choy, "New zero-current transition PWM DC/DC converters without current stress," *IEEE Trans. Power Electron.*, vol. 18, no. 1, pp. 95-104, Jan. 2003.
- [5] H. Wannian, G. Xing, S. Bassan, and G. Moschopoulos, "Novel dual auxiliary circuits for ZVT-PWM converters," *Can. J. Electr. Comput. Eng.*, vol. 33, pp. 153-160, Summer-Fall 2008.
- [6] G. Hua, C. S. Leu, Y. Jiang, and F. C. Lee, "Novel zero-voltage-transition PWM converters," *IEEE Trans. Power Electron.* vol. 9, no. 2, pp. 213-219, Mar. 1994.
- [7] G. Hua, E. X. Yang, Y. Jiang, and F. C. Lee, "Novel zero-current-transition PWM converters," *IEEE Trans. Power Electron.*, vol. 9, pp. 601-606, Nov. 1994.
- [8] H. Mao, F. C. Lee, X. Zhou, H. Dai, M. Cosan, and D. Boroyevich, "Improved zero-current-transition converters for high-power applications," *IEEE Trans. Ind. Appl.*, vol. 33, no. 5, pp. 1220-1232, Sep./Oct. 1997.
- [9] C. J. Tseng and C. L. Chen, "Novel ZVT-PWM converters with active snubbers," *IEEE Trans. Power Electron.* vol. 13, no. 5, pp. 861-869, Sep. 1998.
- [10] W. Li, Y. Zhao, Y. Deng, and X. He, "Interleaved converter with voltage multiplier cell for high step-up and high-efficiency conversion," *IEEE Trans. Power Electron.*, vol. 25, no. 9, pp. 2397-2408, Sep. 2010.
- [11] D. Y. Jung, Y.-H. Ji, S.-H. Park, Y.-C. Jung and C.-Y. Won "Interleaved soft-switching boost converter for photovoltaic power-generation system", *IEEE Trans. Power Electron.*, vol. 26, no. 4, pp.1137 -1145 2011.
- [12] T. Chen, S. Shiu and R. Liang "Analysis and design of a zero-voltage-switching and zero-current- interleaved boost converter", *IEEE Trans. Power Electron.*, vol. 27, no. 1, pp.161 -173 2012.
- [13] T. Mishima, Y. Takeuchi and M. Nakaoka "Analysis, design, and performance evaluations of an edge-resonant switched capacitor cell-assisted soft-switching PWM boost DC-DC converter and its interleaved topology", *IEEE Trans. Power Electron.*, vol. 28, no. 7, pp.3363 -3378 2013.
- [14] Hsieh.T.-C. Hsueh and H.-C. Yen "An interleaved boost converter with zero-voltage transition", *IEEE Trans. Power Electron.*, vol. 24, no. 4, pp.973 -978 2009.